Zeitschrift für Kristallographie 150, 299–320 (1979)

The crystal structures of low chalcocite and djurleite*

Howard T. Evans, Jr.

U.S. Geological Survey, National Center 959, Reston, Virginia 22092, USA

Received: March 19, 1979

Abstract. Low chalcocite is monoclinic, space group $P2_1/c$, with a unit cell having $a = 15.246(4)$ Å, $b = 11.884(2)$ Å, $c = 13.494(3)$ Å, $\beta = 116.35(1)°$, and containing 48 Cu_2S. Its structure was solved by the symbolic addition method, using 5155 independent intensity data measured with Mo$K\alpha$ radiation on an automatic diffractometer. Refinement in anisotropic mode led to $R = 0.086$. The structure is based on hexagonal-close-packed framework of sulfur atoms, with copper atoms occupying mainly triangular interstices. Of the 24 different copper atoms, 21 form triangular CuS_3 groups, and one is in a distorted CuS_4 tetrahedron.

Djurleite is monoclinic, space group $P2_1/n$, with a unit cell having $a = 26.897(6)$ Å, $b = 15.745(3)$ Å, $c = 13.565(3)$ Å, $\beta = 90.13(3)°$, and containing 8 $Cu_{31}S_{16}$. The structure was solved by extending the known substructure phases by the symbolic addition procedure, using 5686 independent intensity data measured with Mo$K\alpha$ radiation. Refinement converged at $R = 0.116$. The structure is similar in general to the low chalcocite structure, but of the 62 different copper atoms, 52 form triangular groups, 9 form distorted tetrahedral groups, and one is in unique linear twofold coordination.

Both structures are derived from the high chalcocite structure ($P6_3/mmc$, $a = 3.96$ Å, $c = 6.72$ Å, cell content = 2 Cu_2S) which forms a substructure corresponding to the hexagonal-close-packed sulfur framework, but the details of the copper arrangement are entirely different in the two phases. The average Cu–S bond length in the CuS_3 triangles is 2.32 Å in low chalcocite and 2.29 Å in djurleite. The overall average Cu–S distance in the tetrahedra is 2.48 Å, but varies from 2.22 to 2.91 Å. Each copper atom has from 2 to 8 other copper atom neighbors less than 3.0 Å distant, varying up from 2.45 Å through a maximum clustering at about 2.78 Å. Cu–Cu bonding interaction is probably significant but is not clearly understood.

---

* Dedicated to Prof. W. Nowacki on occasion of his 70th birthday

Introduction

Several major detailed studies of the Cu–S system have been published (Roseboom, 1966; Rau, 1967; Cook, 1972; Potter, 1977), all of which show the existence of two phases Cu_xS at room temperature with x close to 2. The stoichiometric phase Cu_2S has long been known as chalcocite, a supergene or hypergene ore mineral of copper. The existence of the compositionally close-lying phase having $x = 1.96$ was discovered in an X-ray study of the Cu–S system by Djurle (1958), and soon became recognized as a mineral which was named in his honor (Roseboom, 1962; Morimoto, 1962). Mathieu and Rickert (1972), and Potter (1977), in careful electrochemical studies, showed that (low) chalcocite at room temperature has a very narrow homogeneity range, in which x lies between 1.997 and 2.000 ($\pm$ 0.002). The range is considerably broader for djurleite, as x ranges between 1.934 to 1.965 $\pm$ 0.002. The low-temperature form of chalcocite, commonly designated "low chalcocite", and djurleite both revert on heating to the disordered hexagonal phase called "high chalcocite", the former at 103.5° C, the latter at 93° C.

Both low chalcocite and djurleite are very common species, often intermixed or intergrown. Many specimens in museums and study collections labelled "chalcocite" may actually be primarily djurleite. A comprehensive study of the crystal habits of the two minerals has not yet been made, but the author's experience suggests that the elongated prismatic habit of crystals from Bristol, Connecticut is characteristic of low chalcocite, and that the flat, hexagonal, platy habit bounded by prisms that is common at Redruth, Cornwall, is characteristic of djurleite. Their physical and optical properties are practically identical. Thus, the only certain method to distinguish the two is X-ray diffraction (Roseboom, 1966).

The structures of both low chalcocite and djurleite are based on a hexagonal-close-packed framework of sulfur atoms, with the copper atoms arranged in a complex way in the interstices. At about 100° C the copper atoms become highly disordered, virtually "fluid", with the transformation to high chalcocite, for which the crystallography, as Ueda (1949) first showed, is simply that of the sulfur framework itself. The high mobility of copper in this phase is associated with unusually high ionic conductivity, as shown by Hirahara (1951). When the copper atoms "freeze" on cooling in a sharp, first-order transition, they become fixed in either the low chalcocite or the djurleite arrangement, presumably depending on the local Cu/S proportions at the point of nucleation, although Putnis (1976) claimed that one or the other may appear at random at stoichiometric composition. Knowledge of the details of the copper arrangement in the low temperature phases has naturally been much desired as new aspects of the complex Cu–S system have been discovered. Both structures have now been solved by the author in this laboratory, and their structure analyses and the resulting

detailed atomic arrangements are described in this paper. Preliminary notices of these findings have been published previously (Evans, 1971; Evans, 1979).

Previous crystallographic studies

The proper pseudo-orthorhombic cell of low chalcocite was first determined by Rahlfs (1936). A detailed analysis of the crystallography of this phase was then reported by Buerger and Buerger (1944), who established an A-centered orthorhombic cell with $a = 11.92$ Å, $b = 27.84$ Å and $c = 13.44$ Å, containing 96 Cu_2S. Assuming that the crystal is orthorhombic, they showed that the space group $A\,b\,2m$ is the only one compatible with the hexagonal unit cell of high chalcocite, from which it is most probably derived as a superstructure produced by small atomic displacements. However, the nature of this superstructure has remained hidden until the present study.

The first insight into the structure of high chalcocite was given by Ueda (1949), who showed that an approximate explanation of the observed X-ray intensities is obtained on the basis of two sulfur atoms in the cell in hexagonal closest packing, with no regard to the copper atoms. It became clear that this hexagonal-close-packed sulfur framework prevails also in low chalcocite, associated with the pseudohexagonal character observed by Buerger and Buerger (1944). Eventually, by careful electron density study of the high chalcocite cell, Wuensch and Buerger (1963) and also Koto and Morimoto (1965) found that the sulfur framework is sharply delineated, but that the copper atoms are highly disordered, being smeared out through the interstices, with some concentration at triangular, tetrahedral and linear coordination sites.

As mentioned above, djurleite was first recognized in an X-ray study by Djurle (1958), who assigned to it an orthorhombic cell in space group *Pmnm* containing 128 Cu_xS where $x = 1.96$. A detailed study of the crystallography of this phase, which is complicated by extensive twinning (Takeda, Donnay and Appleman, 1967), was made by Takeda, Donnay, Roseboom and Appleman (1967). They showed clearly how the superstructure relationship between high and low chalcocite extends also to djurleite, which has a pseudohexagonal character even stronger than that of low chalcocite. These authors listed an orthorhombic cell like that of Djurle (1958), but expressed the strong feeling that the phase may actually be monoclinic in space group $P2_1/n$. The present author had the privilege of examining their precession photographs, from which it was possible to reach this conclusion unequivocally. With the later discovery of untwinned crystals, the fact was dramatically confirmed.

Crystallographic metrics of chalcocite and djurleite

The unit cell dimensions of chalcocite and djurleite were determined by means of least squares analysis of X-ray powder data obtained from the Hägg-Guinier focussing camera. The method and resulting powder data have been presented by Potter and Evans (1976). The unit cells obtained are given in Table 1, which is analogous to Table 2 of Takeda, Donnay, Roseboom and Appleman (1967). For low chalcocite, a crystal from Bristol, Connecticut was used for the powder run and all subsequent single crystal work. The composition is assumed to be essentially invariant at Cu_2S. The full set of single crystal intensity data were available to enable Potter and Evans to index the powder pattern unambiguously on the monoclinic cell. This was not the case for djurleite at that time, so they assumed an orthorhombic cell. Also, the sample of djurleite from the Ozark Lead Co. mine at Sweetwater, Missouri, that was used for the powder pattern (and also the subsequent

Table 1. Unit cells of high chalcocite, low chalcocite, and djurleite

Parameter	High chalcocite[a]	Low chalcocite		Djurleite
		ps.-ortho.[b]	monoclinic	
Space group	$P6_3/mmc$	$A2_1/c11$	$P2_1/c$	$P2_1/n$
a, Å	$\left\{\begin{matrix} a_{cch}{}^{c} \\ 3.961(4) \end{matrix}\right.$	$a_{cco}{}^{c} \sim 3\,a_{cch}$ 11.884(2)	$a_{ccm}{}^{c} = [0,\frac{1}{2},\frac{\bar{1}}{2}]_{cco}$ 15.246(4)	$a_{dj}{}^{c} \sim 4\,c_{cch}$ 26.897(6)
b, Å	$\left\{\begin{matrix} b_{cch} \\ 6.861(6) \end{matrix}\right.$	$b_{cco} \sim 4\,b_{cch}$ 27.324(4)	$b_{ccm} = a_{cco}$ 11.884(2)	$b_{dj}{}^{c} \sim 4\,a_{cch}$ 15.745(3)
c, Å	$\left\{\begin{matrix} c_{cch} \\ 6.722(7) \end{matrix}\right.$	$c_{cco} \sim 2\,c_{cch}$ 13.494(3)	$c_{ccm} = c_{cco}$ 13.494(3)	$c_{dj} \sim 2\,b_{cch}$ 13.465(3)
β	–	90.08(1)	116.35(1)	90.13(2)
V, Å^{c}	182.7	4382(2)	2190(1)	5744(2)
Cell contents	$2\,Cu_2S$	$96\,Cu_2S$	$48\,Cu_2S$	$8\,Cu_{31}S_{16}$
D_x, gm/cm^3	5.785	5.789		5.740

[a] Orthohexagonal cell at 152°C according to Djurle (1958)
[b] Setting of Buerger and Buerger (1944)
[c] Subscripts: *cch* = high chalcocite; *cco* = low chalcocite, pseudo-orthorhombic setting; *ccm* = low chalcocite, primitive monoclinic setting; *dj* = djurleite

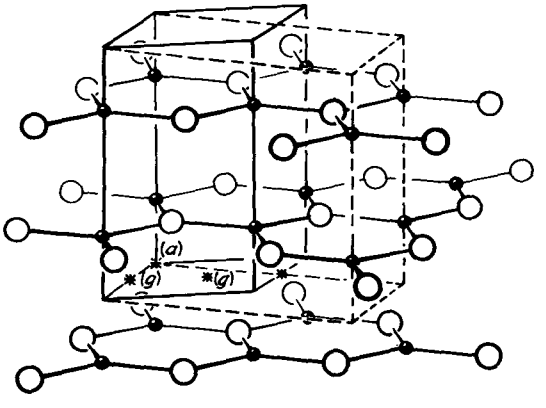

Fig. 1. The partial structure of high chalcocite, showing the characteristic CuS layers. Centers of symmetry are indicated by (*a*) and (*g*). Dashed lines show orthohexagonal unit cell

single crystal study), has a composition that was not precisely known. Both deficiencies have now been filled: the pattern can be unambiguously indexed on the monoclinic cell, and the composition is $Cu_{1.938}S$. The unit cell given for djurleite in Table 1 is slightly modified by this refinement with respect to that given by Potter and Evans (1976).

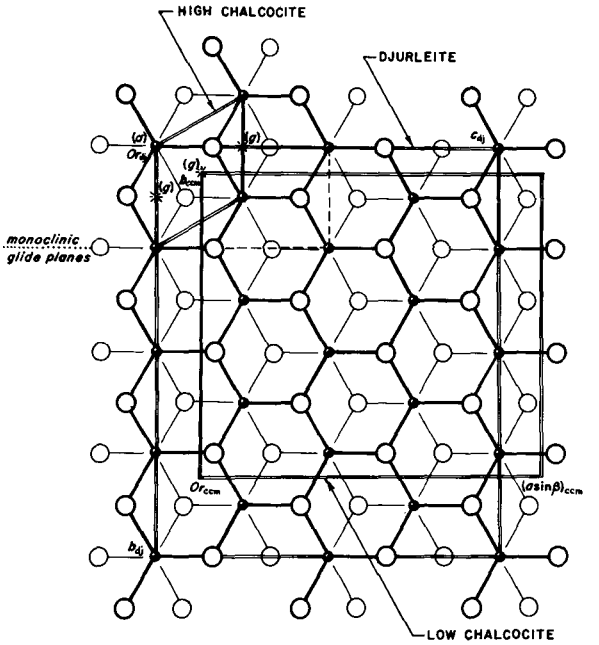

Fig. 2. View normal to the CuS layers in chalcocite and djurleite, showing relationships among the unit cells of high chalcocite, monoclinic low chalcocite (*ccm*) and djurleite (*dj*)

The direct cell transformations for vectors **X** (x,y,z) among the various lattices of hexagonal high chalcocite (*cch*), pseudo-orthorhombic low chalcocite (*cco*), monoclinic low chalcocite (*ccm*) and djurleite (*dj*) in the settings shown in Fig. 2 are given by the following matrices:

	← Left	→ Right
$\mathbf{X}_{cch} \leftrightarrow \mathbf{X}_{cco}$	$\begin{pmatrix} 3 & 4 & 0 \\ 0 & 8 & 0 \\ 0 & 0 & 2 \end{pmatrix}$	$\begin{pmatrix} \frac{1}{3} & -\frac{1}{6} & 0 \\ 0 & \frac{1}{8} & 0 \\ 0 & 0 & \frac{1}{2} \end{pmatrix}$
$\mathbf{X}_{cco} \leftrightarrow \mathbf{X}_{ccm}$	$\begin{pmatrix} 0 & 1 & 0 \\ \frac{1}{2} & 0 & 0 \\ -\frac{1}{2} & 0 & 1 \end{pmatrix}$	$\begin{pmatrix} 0 & 2 & 0 \\ -1 & 0 & 0 \\ 0 & 1 & 1 \end{pmatrix}$
$\mathbf{X}_{cch} \leftrightarrow \mathbf{X}_{ccm}$	$\begin{pmatrix} 2 & -3 & 0 \\ 4 & 0 & 0 \\ -1 & 0 & 2 \end{pmatrix}$	$\begin{pmatrix} 0 & \frac{1}{4} & 0 \\ -\frac{1}{3} & \frac{1}{6} & 0 \\ 0 & \frac{1}{8} & \frac{1}{2} \end{pmatrix}$
$\mathbf{X}_{cch} \leftrightarrow \mathbf{X}_{dj}$	$\begin{pmatrix} 0 & 4 & 0 \\ 0 & 0 & 2 \\ 4 & 0 & 0 \end{pmatrix}$	$\begin{pmatrix} 0 & 0 & \frac{1}{4} \\ \frac{1}{4} & 0 & 0 \\ 0 & -\frac{1}{2} & 0 \end{pmatrix}$

The reciprocal cell transformations for vectors **H** (*hkl*) are obtained by transposing these matrices and exchanging left for right.

An important element in these structures consists of the layer of sulfur atoms in the hexagonal-close-packed framework, in which half of the triangle centers are occupied alternately by copper atoms. Figure 1 shows the unit cell of high chalcocite with these layers depicted. Actually at 125° C Wuensch and Buerger (1963) found that the copper sites are only 85% occupied, and Sadanaga, Ohmasa and Morimoto (1965) found even lower occupancies at other temperatures. Fully occupied layers with composition CuS are present in covellite, CuS (Evans and Konnert, 1976), and stromeyerite, AgCuS (Frueh, 1955). The centered orthohexagonal cell is shown by dashed lines in Figs. 1 and 2 to emphasize its relation to the supercells. In Fig. 2 a view normal to these layers is shown in which the rational supercell relationships to the hexagonal subcell defined in Table 1 are outlined. The centers of symmetry in the high chalcocite cell are at 2 (*a*), (0,0,0; 0,0,$\frac{1}{2}$), and at 6 (*g*) ($\frac{1}{2}$,0,0; 0,$\frac{1}{2}$,0; $\frac{1}{2}$,$\frac{1}{2}$,0; $\frac{1}{2}$,0,$\frac{1}{2}$; 0,$\frac{1}{2}$,$\frac{1}{2}$; $\frac{1}{2}$,$\frac{1}{2}$,$\frac{1}{2}$) in the space group $P6_3/mmc$. In approaching the structure problem for low chalcocite and djurleite, we will try to place the origin of the supercell on one of these points.

Both the supercells have their unique *b* axes parallel to the hexagonal *a* axis of high chalcocite. The CuS layers are then normal to *c* in low chalcocite and normal to *a* in djurleite. An additional restriction on the relationship of the supercells to the subcell derives from the fact that the glide planes in the former must coincide with the mirror planes of the latter, and that the sulfur atoms must lie in or close to these glide planes. Thus, as Buerger and Buerger (1946) found by a more formal method, there can be no mirror plane normal to the glide plane and parallel to the pseudohexagonal *c* axis in low chalcocite, which means that if low chalcocite were orthorhombic it would have to be noncentrosymmetric. Now that we know that the supercells are monoclinic the last conclusion does not hold, and we may assume the space groups $P2_1/c$ or $P2_1/n$.

The restriction on the location of glide planes critically affects the possible (*a*) or (*g*) sites that are permissible for the origin of the supercells. Referring to the horizontal rows of sulfur atoms in Fig. 2 (normal to the hexagonal *a* axis direction), because the *b* axis of low chalcocite is 3 times the hexagonal *a* axis, and sulfur atoms must lie in the monoclinic glide planes at $y_{ccm} = \frac{1}{4}$ and $\frac{3}{4}$, the origin in low chalcocite can only lie halfway between the sulfur rows, that is, at the hexagonal (*g*) site at $\frac{1}{2},\frac{1}{2},0$ (or $0,\frac{1}{2},0$). An ambiguity still remains, on the question as to whether the positive direction of the monoclinic *a* axis lies to the right or to the left in Fig. 2. For djurleite, where the monoclinic *b* axis is 4 times the hexagonal *a* axis, the origin must lie in the sulfur rows, and may be located at the site (*a*) 0,0,0, or at the site (*g*) $\frac{1}{2}$,0,0. For each of these possible sites, the ambiguity with respect to the positive *a* axis direction also obtains.

As it happened, the structure of low chalcocite was solved directly by the symbolic addition procedure without regard to the above possible am-

biguities. In the case of djurleite, where the subcell reflections were considerably more dominant than in the case of low chalcocite, a strategy was required that examined each possible origin in turn. It should be observed that while we speak here of superstructures based on a simple substructure, the superstructure is not the displacive kind in which the larger structure is derived from small displacements of atoms from ideal or symmetrical positions in the substructure. Rather, the superstructure results from an ordering in particular sites of atoms which in the substructure are completely disordered over long distances. Thus, the special techniques for the solution of displacive type superstructures that have been developed in recent years cannot be applied in the case of chalcocite and djurleite. Also, because there are no fixed groups in these structures we cannot use any predetermined structural restraints in the solution or refinement of these structures. For example, although we may expect to find many CuS_3 triangular groups, the Cu−S and S−S distances may vary over a wide range, and cannot be constrained.

Structure analysis of low chalcocite

Many crystals were examined in a search for one suitable for structure analysis, but most either showed adverse twinning or proved to be mainly djurleite. The best material seemed to be that from the classical locality at Bristol, Connecticut. A large fragment was crushed in a steel mortar under liquid nitrogen to prevent any plastic deformation. Several of these anhedral crystals were examined by the precession method, always on the lookout (for no good reason) for monoclinic symmetry in the centered nets. Finally one was found that showed such lowered symmetry in a series of *hkn* patterns (mirror but no axial symmetry on upper levels), although strongly pseudo-orthorhombic, at least on the even lattice levels. The odd levels, which were considerably weaker than the even levels, showed clear monoclinic symmetry with no apparent pseudosymmetry. In fact, certain reflections such as $\bar{4}41$ (orthorhombic $\overline{471}$) appeared moderately strong while the corresponding 341 reflection (orthorhombic $\bar{4}71$) was nearly absent. Thus it was concluded that the incipient twinning on (100) that is nearly universal in larger crystals was absent in this specimen. It was irregular but roughly pyramidal in shape, with a base 0.20 × 0.11 mm and height 0.08 mm. The base was bounded by (100), which is apparently a poorly developed cleavage plane.

Intensity data were collected with an automated Picker diffractometer, using Nb-filtered Mo$K\alpha$ radiation. A total of 5155 independent reflections with $2\theta \leq 50°$ were measured by $\theta/2\theta$ scan; 2931 of these registered intensities having $F > 3\sigma(F)$. These were corrected in the usual way for Lorentz and polarization effects, and then normalized to E values, at this stage without absorption corrections. The statistical distribution of the E values strongly indicated centrosymmetry, which was assumed in the solution of the structure. The largest value was 6.62 for 494 and the highest 14 reflections were substructure reflections. The highest nonsubstructure E value was 4.00 for 13.3.2. The origin was established by setting E's positive for 494, 13.3.2, and 295 ($E = 3.00$). Phases were then developed by hand using the symbolic addition procedure for ~360 terms ($E > 1.50$). The process was smooth except for a group of reflections related to 1.8.10 ($E = 3.90$) for which an absolute phase could not be determined. Thus, a twofold ambiguity arose requiring two trial Fourier maps. Both E maps contained large numbers of prominent peaks in addition to those clearly associated with the hexagonal-close-packed sulfur framework, but for one these extra peaks were fairly uniform in height, arranged without unreasonably close contacts, and accounted well for the expected 24 copper atoms. The other map was far less well resolved, with many distorted and unreasonably closely spaced peaks. Thus, only the first choice was acceptable.

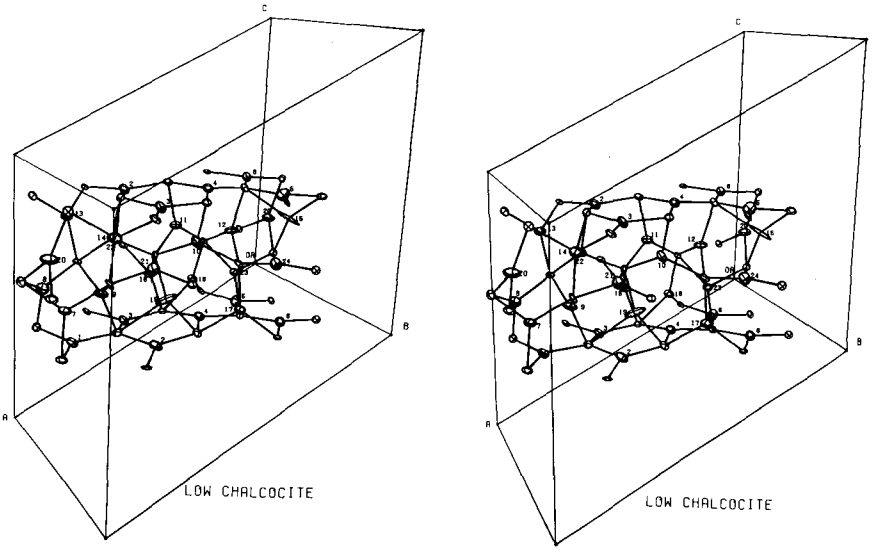

Fig. 3. Stereoscopic projection of a portion of the crystal structure of low chalcocite, showing the thermal ellipsoids at the 50 % probability envelope. All copper atoms are numbered

An initial structure based on 24 Cu and 12 S atoms derived from the E map with overall $B = 1.0$ (109 parameters) gave a conventional reliability index $R = 0.42$ for 3288 data with $F > 2\sigma(F)$. In isotropic thermal mode (145 parameters) R was reduced to 0.163 after 9 cycles, and in anisotropic mode (324 parameters) to 0.118 after 6 more cycles. After several more trials, in which anomalous dispersion corrections were included and the data set reduced to 2897 with $F > 3\sigma(F)$ (with 34 strong reflections excluded for obvious extinction effects), but still with no absorption corrections and unit weights applied, R reached 0.108, and difficulties with nonpositive definite atoms were eliminated. At this point an ellipsoid drawing of the structure was prepared, which is shown in Fig. 3. The only unusual thermal anisotropies that appeared were those associated with Cu(15) and Cu(19). These were extremely elongated, suggesting some ambiguity about the coordination of these atoms, that is, something missing from the assumed model.

The suggestion is that Cu(15) and Cu(19) may each equally well lie in two possible sites, and this behavior may be accounted for either by letting each lie half time in each site, disordered in the same centrosymmetric space group; or a lower symmetry group (Pc or $P2_1$) may be assumed and the various sites occupied in an ordered way. A refinement was first attempted based on the split-atom model in $P2_1/c$, but this did not lead to any improvement in the reliability index. In this process, Cu(15) split into two half atoms separated by 0.62 Å with reasonable thermal motions, but the Cu(19) pair became only 0.2 Å apart and nonpositive definite. In the space group Pc, starting with the best model in $P2_1/c$ but with the atom pairs appropriately displaced, refinement was pursued with a reduction of R by about 0.2, but many atoms became nonpositive definite, many correlation coefficients ran over 0.95, and parameter errors became 3 or 4 times those obtained in the centrosymmetric refinement. After much effort was thus applied to refine a structure based on small displacements of atoms from the first centrosymmetric model in $P2_1/c$, all such attempts were abandoned as fruitless.

A closely similar situation was found recently by Lewis and Kupčík (1974) in the synthetic compound $Bi_2Cu_3S_4Cl$. One of the three kinds of copper atoms in the structure they determined

Table 2. Structure parameters for low chalcocite. $\sigma(x) = \sigma(y) = \sigma(z) = 0.0006$ for S, 0.0004 for Cu

Atom	x	y	z	$\bar{u}_{rms}$, Å	Atom	x	y	z	$\bar{u}_{rms}$, Å
S(1)	0.9575	0.0829	0.8422	0.13	Cu(7)	0.9345	0.1233	0.9923	0.17
S(2)	0.9413	0.0768	0.3462	0.12	Cu(8)	0.9414	0.1412	0.5099	0.17
S(3)	0.7940	0.0824	0.5068	0.10	Cu(9)	0.7615	0.2504	0.4109	0.17
S(4)	0.7917	0.0817	0.0060	0.12	Cu(10)	0.4429	0.1477	0.9348	0.16
S(5)	0.4491	0.0883	0.6133	0.12	Cu(11)	0.4254	0.1229	0.4388	0.15
S(6)	0.4444	0.0726	0.0957	0.12	Cu(12)	0.2578	0.2357	0.8507	0.17
S(7)	0.2999	0.0781	0.7868	0.12	Cu(13)	0.8209	0.0358	0.6830	0.15
S(8)	0.2843	0.0832	0.2869	0.11	Cu(14)	0.7830	0.0624	0.1671	0.18
S(9)	0.6960	0.2481	0.7220	0.13	Cu(15)	0.0261	0.2045	0.7722	0.26
S(10)	0.5479	0.2237	0.4167	0.11	Cu(16)	0.5026	0.0795	0.2834	0.16
S(11)	0.1970	0.2384	0.4766	0.12	Cu(17)	0.3022	0.0434	0.6230	0.19
S(12)	0.0483	0.2324	0.1332	0.12	Cu(18)	0.3050	0.0431	0.1339	0.16
Cu(1)	0.8645	0.2496	0.2927	0.15	Cu(19)	0.5243	0.2082	0.7543	0.24
Cu(2)	0.6171	0.0740	0.6765	0.16	Cu(20)	0.9992	0.0856	0.2166	0.18
Cu(3)	0.6102	0.0916	0.1677	0.15	Cu(21)	0.6227	0.1032	0.9531	0.16
Cu(4)	0.3628	0.2400	0.0731	0.14	Cu(22)	0.7037	0.1944	0.5659	0.17
Cu(5)	0.1276	0.0849	0.9451	0.18	Cu(23)	0.2028	0.2069	0.1398	0.17
Cu(6)	0.1065	0.0783	0.4429	0.15	Cu(24)	0.1308	0.0966	0.6791	0.17

(in space group $P2_12_12_1$) showed an extremely elongated ellipsoid. When they assumed this atom to be divided into two half-occupied positions, refinement placed them in two adjacent sites 0.63 Å apart, one in triangular coordination and one in linear coordination. The other two kinds of copper atoms were found to be in tetrahedral coordination.

Late in the refinement stages an absorption correction was applied by bounding the conchoidal fracture surfaces of the crystal by 8 planes. The linear absorption coefficient for Mo$K\alpha$ was 238 cm^{-1}, and the transmission factors varied from 0.136 to 0.378. An isotropic extinction factor was also incorporated, with the strong reflections included. Final block refinement of the 36-atom model, with the data weighted according to $1/\sigma(F)$ as obtained from counting statistics, yielded $R = 0.086$ and R_w [based on $w\Delta(F^2)] = 0.056$. The resulting structure parameters are given in Table 2 and the thermal parameters are given in Table 3. A list of observed and calculated structure factors may be obtained on request from the author.

For all the calculations referred to above (and also those for djurleite), extensive use was made of the computer programs of the XRAY 76 system edited and written by James M. Stewart of the University of Maryland, and RFINE written by Larry W. Finger of the Geophysical Laboratory. Stereoscopic graphics were produced with ORTEP written by Carroll K. Johnson of the Oak Ridge National Laboratory. The computations were executed on IBM 370/155 and Honeywell 60/68 (with MULTICS) systems. Atomic scattering factors for neutral Cu and S as represented analytically by Doyle and Turner (1968) were used throughout. The anomalous dispersion factors and mass absorption coefficients of Cromer and Liberman (1970) were used in the treatment of the data.

Structure analysis of djurleite

As in the case of low chalcocite, the structure of djurleite could not be studied until truly single, untwinned crystals could be obtained. Such crystals became available recently from a specimen

Table 3. Anisotropic thermal parameters for low chalcocite U(Å) in exp $[-2\pi^2 (U_{11}h^2 a^{*2} + U_{22}k^2 b^{*2} + U_{33}l^2 c^{*2} + 2U_{12}hka^* b^* + 2U_{13}hla^* c^* + 2U_{23}klb^* c^*)]$. Tabulated values are $U \times 1000$; $\sigma(U) = 0.005$ for S, 0.003 for Cu

Atom	U_{11}	U_{22}	U_{33}	U_{12}	U_{13}	U_{23}	Atom	U_{11}	U_{22}	U_{33}	U_{12}	U_{13}	U_{23}
S(1)	18	22	17	8	10	−2	Cu(7)	34	41	22	−7	20	−5
S(2)	16	10	17	2	8	1	Cu(8)	31	25	27	−5	14	−3
S(3)	16	11	9	−1	9	−1	Cu(9)	45	24	30	−1	29	1
S(4)	13	15	26	−4	15	1	Cu(10)	23	26	37	−1	20	3
S(5)	20	11	20	−3	14	3	Cu(11)	32	22	20	−6	15	−1
S(6)	15	22	10	−1	6	2	Cu(12)	41	28	22	8	21	−4
S(7)	18	13	23	0	17	−1	Cu(13)	32	24	19	2	14	1
S(8)	15	17	9	5	9	−3	Cu(14)	39	43	23	−9	19	4
S(9)	14	21	11	5	4	1	Cu(15)	103	59	106	48	101	60
S(10)	10	13	14	4	4	1	Cu(16)	37	28	20	−3	19	1
S(11)	14	14	14	−1	9	−5	Cu(17)	43	51	23	−21	24	−11
S(12)	14	16	17	0	7	2	Cu(18)	34	27	21	7	20	−3
Cu(1)	25	18	30	−3	18	−2	Cu(19)	92	48	21	27	11	−11
Cu(2)	30	18	35	8	24	6	Cu(20)	54	26	29	2	30	2
Cu(3)	20	24	33	−1	17	0	Cu(21)	25	15	34	8	15	1
Cu(4)	24	18	25	−1	15	−2	Cu(22)	38	36	25	19	24	9
Cu(5)	36	20	35	6	13	0	Cu(23)	40	38	20	19	22	7
Cu(6)	21	24	27	2	12	0	Cu(24)	30	17	39	4	17	5

obtained from the Ozark Lead Co. mine near Sweetwater, Missouri. These crystals grow as thin plates which tend to coalesce to form larger mosaic crystals aggregates. The freshest, thin crystals [plates parallel to (100)] were found to consist of single, untwinned individuals up to 5 mm wide. The crystal selected for intensity measurement was a flake of irregular outline, approximately 0.6 × 0.3 mm in size and 0.025 mm thick. It may be noted that the appearance of these untwinned crystals in this ore sample indicates that they were formed at a temperature below 95° C, the transition temperature to high chalcocite, because djurleite formed by cooling through this temperature would be filled with twinning.

Intensity data were collected as for chalcocite with the automated Picker diffractometer, using Mo$K\alpha$ radiation. Within the range $2\theta = 4°$ to 45°, 8494 reflections were measured, of which 5686 independent reflections having F values $> 3\sigma(F)$ were established as the working data set. Absorption corrections were calculated ($\mu = 230\,\text{cm}^{-1}$) on the basis of a thin plate parallel to (100) bounded by 5 additional planes. The usual Lorentz and polarization factors were applied, and the resulting structure amplitudes were normalized to E values. The E averages strongly implied a centrosymmetric structure, and the space group $P2_1/n$ was assumed in the structure determination.

The largest E value (for 046) is 11.72, and the highest 48 E values belong to substructure reflections. As explained earlier, there are two possible choices of origin on symmetry centers in the hexagonal-close-packed sulfur framework, and for each the positive monoclinic superstructure a axis may lie either in the [120] or the [$1\bar{2}0$] direction. For each of these four models the phases of the strong substructure reflections are predetermined. In this case, where the substructure is so prominent, the application of the symbolic addition procedure must be initiated separately for each of the four models. This strategy was developed during the actual treatment of the structure problem, and its validity became more and more apparent as the process advanced.

The process was begun by choosing an origin at (*g*) $\frac{1}{2},0,0$ and the *a* axis along [120]. The substructure phases were calculated by hand and the origin in the superstructure was established by setting positive the *E* values of $\overline{11}.5.7$ ($E = 4.13$), $\bar{5}.11.6$ (3.44), and $\overline{10}.1.10$ (2.73). These phases were then extended by the symbolic addition method, by hand to 150 phases, and by computer to 486 phases ($E > 1.6$). The phase of 4.12.0 (not a substructure reflection) could not be found and the body of reflections related to this reflection remained ambiguous. Two *E* maps were therefore synthesized for study. Sections were calculated normal to [100] at levels $x = 3$ and 9 48ths, which contain the two different sulfur layers in the structure between 0 and $\frac{1}{4}$, and at $x = 1, 5, 7$, and 11 48ths, which lie $\frac{1}{3}$ and $\frac{2}{3}$ of the distances between the sulfur layers where the copper atoms would be expected to lie. Both *E* maps were rich in detail, showing clearly the sulfur framework and many inter- and intra-layer peaks at appropriate sites for copper atoms. In one of the maps the interlayer peaks were supernumerous and generally weak in appearance, while the other map showed these Cu peaks in approximately the right number and strongly developed, though sometimes distorted or even split between two possible sites. Starting from the latter map as the most probable image of the structure, structure factors and Fourier maps were calculated through several cycles in an attempt to establish a model that would converge in the refinement process. Finally it became clear that the least squares procedure would not lead to any better structure based on this substructure orientation than one having $R = 0.50$.

The remaining three substructure orientations were then calculated and analyzed in turn in the same way. For each one, the 4.12.0 reflection remained ambiguous, so that in all, 8 different *E* maps were synthesized. Of these only one led to a structure that would refine below $R = 0.50$. This one, the last in the series examined, with origin at (*a*) 0,0,0 in the high chalcocite unit cell (between two intralayer copper atoms), yielded a structure that quickly refined to $R = 0.22$ in 3 least squares cycles, and produced a sharp, clean electron density map having no distortions or spurious features (except for two small peaks). There was no doubt at this point that the correct structure had been found. A count of the atoms turned up the expected 32 sulfur atoms in the assymmetric unit, but only 61 copper atoms, corresponding to an unexpectedly low value of $x = 1.906$ in Cu_xS. It was noticed that the two small peaks both appeared at $y,z = 0.262, 0.245$ on interlayer maps at $x = 5$ and 7 48ths. A section calculated at $x = 6$ 48ths revealed another Cu atom at this location, in an unusual, twofold, linear coordination with sulfur atoms. Sections calculated at additional levels did not turn up any further copper atoms.

Thus, a complete structure was found containing 32 S and 62 Cu in the asymmetric unit, corresponding to $x = 1.9375$ in the formula. This is just at the low end of the homogeneity range of 1.93 to 1.96 determined by Potter (1977). If one additional Cu atom were included the Cu/S ratio would be 1.9688, just at the upper end in this range. The inference is that there is room in this structure somewhere for the 63rd Cu atom, but no trace of it could be found in this structure analysis.

Block refinement was continued through isotropic thermal mode (379 parameters) to $R = 0.149$, and anisotropic mode (849 parameters) to $R = 0.116$. In the last stages the data were weighted according to $1/\sigma(F)$, and the final second order factor $R_w = 0.088$. Certain of the sulfur atoms [S(1,2,9,19,23,30)] became formally nonpositive definite, but not by a significant amount since the tensors could be made positive definite by adjustments of U_{ij} amounting to less than $2\sigma(U)$. The final structure parameters are given in Table 4 and the thermal parameters are given in Table 5. A list of observed and calculated structure factors may be obtained from the author on request.

Crystal structures of low chalcocite and djurleite

The crystal structures of low chalcocite and djurleite contain altogether 96 different copper atoms. The general character of the copper environment is very similar in both, with triangular, threefold coordination prevailing. All of the Cu – S distances less than 3.0 Å are listed in Table 6 for low chalcocite

Table 4. Structure parameters for djurleite. $\sigma(x) = 0.0004$ for S, 0.0002 for Cu; $\sigma(y) = 0.0005$ for S, 0.0003 for Cu; $\sigma(z) = 0.0006$ for S, 0.0004 for Cu

Atom	x	y	z	$\bar{u}_{rms}$, Å	Atom	x	y	z	$\bar{u}_{rms}$, Å
S(1)	0.0646	0.9911	0.1743	0.12	Cu(16)	0.1811	0.9987	0.4834	0.17
S(2)	0.0570	0.2567	0.1634	0.12	Cu(17)	0.1943	0.7503	0.4952	0.14
S(3)	0.0587	0.5127	0.1746	0.13	Cu(18)	0.1811	0.1336	0.7549	0.16
S(4)	0.0563	0.7559	0.1747	0.12	Cu(19)	0.1888	0.3852	0.7415	0.16
S(5)	0.0621	0.1167	0.4139	0.13	Cu(20)	0.1928	0.8775	0.7389	0.18
S(6)	0.0569	0.3729	0.4192	0.10	Cu(21)	0.0163	0.1531	0.0663	0.14
S(7)	0.0698	0.6326	0.4114	0.13	Cu(22)	0.0171	0.3905	0.1371	0.15
S(8)	0.0669	0.8637	0.4146	0.12	Cu(23)	0.0183	0.6344	0.1237	0.18
S(9)	0.0569	0.9932	0.6626	0.14	Cu(24)	0.0149	0.8761	0.1242	0.14
S(10)	0.0661	0.2356	0.6666	0.12	Cu(25)	0.0144	0.2896	0.3064	0.14
S(11)	0.0645	0.4904	0.6666	0.13	Cu(26)	0.0159	0.4645	0.3191	0.16
S(12)	0.0683	0.7477	0.6718	0.12	Cu(27)	0.0174	0.7391	0.3335	0.20
S(13)	0.0650	0.1314	0.9276	0.11	Cu(28)	0.0142	0.1045	0.5931	0.18
S(14)	0.0634	0.3742	0.9149	0.12	Cu(29)	0.0105	0.3883	0.5620	0.21
S(15)	0.0617	0.6297	0.9236	0.16	Cu(30)	0.0171	0.8599	0.6332	0.17
S(16)	0.0660	0.8753	0.9031	0.12	Cu(31)	0.0148	0.9668	0.8134	0.14
S(17)	0.1886	0.1291	0.0741	0.13	Cu(32)	0.1082	0.0824	0.0717	0.13
S(18)	0.1872	0.3834	0.0790	0.12	Cu(33)	0.1073	0.3426	0.0630	0.15
S(19)	0.1834	0.6233	0.0801	0.13	Cu(34)	0.1035	0.9110	0.0507	0.13
S(20)	0.1838	0.8700	0.0748	0.13	Cu(35)	0.1077	0.5346	0.3123	0.17
S(21)	0.1889	0.0044	0.3207	0.13	Cu(36)	0.1125	0.7667	0.3268	0.26
S(22)	0.1928	0.2570	0.3414	0.12	Cu(37)	0.1087	0.9573	0.3159	0.16
S(23)	0.1871	0.4951	0.3374	0.13	Cu(38)	0.1077	0.6589	0.5611	0.14
S(24)	0.1950	0.7473	0.3290	0.13	Cu(39)	0.1076	0.8330	0.5580	0.18
S(25)	0.1827	0.1239	0.5768	0.12	Cu(40)	0.1046	0.0074	0.8874	0.15
S(26)	0.1822	0.3780	0.5718	0.15	Cu(41)	0.1074	0.2501	0.8772	0.16
S(27)	0.1900	0.6216	0.5800	0.11	Cu(42)	0.1129	0.4717	0.8340	0.21
S(28)	0.1875	0.8778	0.5755	0.12	Cu(43)	0.1095	0.7748	0.8162	0.16
S(29)	0.1851	0.9989	0.8256	0.14	Cu(44)	0.1390	0.4994	0.1278	0.15
S(30)	0.1882	0.2603	0.8271	0.12	Cu(45)	0.1374	0.7322	0.1483	0.27
S(31)	0.1934	0.5080	0.8370	0.12	Cu(46)	0.1390	0.1700	0.4220	0.20
S(32)	0.1915	0.7528	0.8246	0.14	Cu(47)	0.1398	0.3665	0.4211	0.28
Cu(1)	0.0589	0.4992	0.0020	0.16	Cu(48)	0.1407	0.0056	0.6581	0.16
Cu(2)	0.0630	0.7552	0.0060	0.16	Cu(49)	0.1455	0.2551	0.6101	0.17
Cu(3)	0.0659	0.1286	0.2466	0.15	Cu(50)	0.1445	0.5031	0.6163	0.18
Cu(4)	0.0659	0.9899	0.4944	0.17	Cu(51)	0.1428	0.5976	0.9303	0.26
Cu(5)	0.0558	0.2425	0.4999	0.15	Cu(52)	0.2241	0.2884	0.1861	0.16
Cu(6)	0.0643	0.5085	0.4952	0.17	Cu(53)	0.2298	0.4622	0.1987	0.16
Cu(7)	0.0674	0.1126	0.7593	0.15	Cu(54)	0.2344	0.1381	0.4237	0.25
Cu(8)	0.0616	0.3598	0.7433	0.18	Cu(55)	0.2342	0.3910	0.4078	0.25
Cu(9)	0.0683	0.6155	0.7542	0.14	Cu(56)	0.2311	0.5884	0.4366	0.17
Cu(10)	0.1884	0.9995	0.9979	0.15	Cu(57)	0.2340	0.5409	0.6925	0.16
Cu(11)	0.1931	0.2535	0.9936	0.16	Cu(58)	0.2322	0.7143	0.6814	0.16
Cu(12)	0.1806	0.7459	0.9892	0.25	Cu(59)	0.2306	0.4086	0.9366	0.19
Cu(13)	0.1887	0.1255	0.2389	0.17	Cu(60)	0.2367	0.6345	0.8759	0.21
Cu(14)	0.1946	0.6214	0.2495	0.17	Cu(61)	0.2356	0.8534	0.9122	0.26
Cu(15)	0.1901	0.8706	0.2423	0.13	Cu(62)	0.1277	0.2615	0.2446	0.20

Table 5. Anisotropic thermal parameters for djurleite. U (Å^2 × 1000) as in Table 3; $\sigma(U) = 0.05$ for S, 0.03 for Cu, except as noted

Atom	U_{11}	U_{22}	U_{33}	U_{12}	U_{13}	U_{23}	Atom	U_{11}	U_{22}	U_{33}	U_{12}	U_{13}	U_{23}
S(1)	14	13	17	9	9	−3	Cu(16)	38	24	27	0	13	1
S(2)	16	8	16	−2	13	5	Cu(17)	24	22	13	−2	3	13
S(3)	22	17	10	−8	−2	−3	Cu(18)	36	19	22	−1	2	−2
S(4)	15	20	10	4	4	−3	Cu(19)	46	18	12	0	1	0
S(5)	19	23	12	−6	0	0	Cu(20)	45	17	34	0	0	−1
S(6)	16	6	11	−5	−1	−1	Cu(21)	19	26	18	−2	12	−4
S(7)	22	8	21	5	−4	−5	Cu(22)	23	17	28	−4	16	−4
S(8)	21	5	20	−4	0	−5	Cu(23)	25	20	47	−3	7	7
S(9)	27	12	15	−8	18	1	Cu(24)	12	19	29	−3	3	−2
S(10)	9	20	14	−3	7	−2	Cu(25)	22	19	17	−2	2	3
S(11)	11	4	33	0	6	2	Cu(26)	23	27	27	2	3	5
S(12)	9	11	22	1	13	1	Cu(27)	13	63	45	1	1	11
S(13)	11	10	16	3	6	−3	Cu(28)	22	29	47	7	1	1
S(14)	12	18	15	3	−2	−11	Cu(29)	28	34	73	9	40	23
S(15)	26	46	7	6	−4	1	Cu(30)	17	19	47	3	11	11
S(16)	5	17	18	−4	−5	15	Cu(31)	13	20	23	2	12	5
S(17)	16	23	13	4	5	−5	Cu(32)	17	21	16	2	12	−2
S(18)	14	9	19	2	−2	−2	Cu(33)	20	28	20	−3	5	2
S(19)	17	5	27	−7	11	3	Cu(34)	18	20	17	1	10	−6
S(20)	24	3	24	1	13	5	Cu(35)	14	54	19	1	3	−10
S(21)	21	14	16	−8	1	−3	Cu(36)	14	56	128[a]	5	9	−26
S(22)	17	9	20	3	8	−1	Cu(37)	19	42	18	−1	13	5
S(23)	22	20	11	20	9	6	Cu(38)	25	14	18	0	2	−3
S(24)	18	13	16	−1	0	−1	Cu(39)	23	36	39	3	13	18
S(25)	19	9	16	0	2	−1	Cu(40)	31	19	19	1	4	1
S(26)	42	14	16	−8	2	2	Cu(41)	17	17	40	0	13	−1
S(27)	4	21	14	6	4	−3	Cu(42)	30	46	53	−14	12	−8
S(28)	10	14	17	−5	8	8	Cu(43)	22	29	23	0	4	−9
S(29)	25	23	15	−4	10	−2	Cu(44)	15	30	27	7	14	−5
S(30)	15	13	15	−5	15	−3	Cu(45)	37	105	81	37	3	−32
S(31)	16	10	14	−5	6	−4	Cu(46)	30	40	45	−14	22	3
S(32)	37	6	12	4	4	1	Cu(47)	16	184[a]	35	0	9	−5
Cu(1)	36	22	20	−1	10	−4	Cu(48)	15	28	34	−3	5	−2
Cu(2)	30	24	24	−3	10	6	Cu(49)	27	25	37	−4	7	7
Cu(3)	31	15	21	0	12	−2	Cu(50)	20	20	53	2	4	5
Cu(4)	55	20	16	7	6	−2	Cu(51)	26	108[a]	74	−3	13	−59
Cu(5)	27	18	24	2	9	6	Cu(52)	23	33	24	5	8	7
Cu(6)	35	21	28	−5	2	4	Cu(53)	22	28	25	−1	5	−4
Cu(7)	28	23	13	−3	8	−1	Cu(54)	28	86	67	11	16	10
Cu(8)	52	21	20	−5	1	−5	Cu(55)	19	64	106[a]	9	9	35
Cu(9)	27	15	13	−1	8	1	Cu(56)	15	38	29	−1	5	−3
Cu(10)	25	20	23	2	5	3	Cu(57)	25	29	25	0	0	1
Cu(11)	31	23	19	−1	−2	0	Cu(58)	17	35	21	−2	0	−2
Cu(12)	70[a]	59	53	−5	19	4	Cu(59)	24	43	43	0	15	16
Cu(13)	41	26	22	2	−2	2	Cu(60)	27	37	63	4	5	−15
Cu(14)	33	34	22	2	6	2	Cu(61)	29	109[a]	67	−19	−13	−37
Cu(15)	21	16	14	−3	7	0	Cu(62)	32	36	52	1	−16	9

[a] $\sigma(U) = 0.06$.

Table 6. Cu – S interatomic distances and angles in low chalcocite. All distances less than 3.0 Å listed in increasing order of d. Last column gives the difference of the sum of 3 (largest) angles from full circle. Standard deviation $\sigma(d) = 0.010$ Å, $\sigma(\phi) = 0.4$ deg

Atom	S_1	d_1	S_2	d_2	S_3	d_3	ϕ_{12}	ϕ_{23}	ϕ_{31}	360-$\Sigma\phi$
Cu(1)	9	2.31	2	2.32	1	2.36	117.1	120.1	121.7	1.1
Cu(2)	8	2.31	5	2.32	9	2.33	130.2	112.8	116.8	0.2
Cu(3)	9	2.24	6	2.28	7	2.36	126.8	115.6	117.0	0.7
Cu(4)	6	2.29	11	2.29	5	2.36	124.7	113.4	120.4	1.5
Cu(5)	4	2.27	11	2.30	1	2.34	126.6	114.6	118.7	0.1
Cu(6)	2	2.26	11	2.28	3	2.34	122.8	111.5	124.9	0.8
Cu(7)	1	2.26	4	2.32	12	2.32	123.4	116.2	119.9	0.5
Cu(8)	12	2.30	3	2.33	2	2.34	125.2	106.6	127.1	1.1
Cu(9)	9	2.29	3	2.31	4	2.31	120.7	119.7	119.6	0.0
Cu(10)	10	2.30	6	2.34	7	2.36	129.0	106.2	124.6	0.2
Cu(11)	5	2.26	8	2.27	10	2.35	123.8	118.7	117.2	0.4
Cu(12)	7	2.27	11	2.29	8	2.42	131.9	109.4	118.6	0.0
Cu(13)	1	2.30	3	2.30	8	2.31	125.5	120.8	113.4	0.3
Cu(14)	4	2.25	7	2.34	2	2.55[a]	126.9	101.0	118.3	13.8
Cu(15)	12	2.18	1	2.22	11	2.91	150.4	98.1	108.6	2.9
Cu(16)	6	2.29	5	2.36	10	2.36	119.4	104.8	135.3	0.4
Cu(17)	7	2.26	3	2.28	5	2.36	126.0	114.2	116.0	3.9
Cu(18)	8	2.27	4	2.34	6	2.42	125.2	102.6	130.5	1.7
Cu(19)	10	2.21	5	2.24	9	2.87	150.6	97.6	109.3	2.5
Cu(20)	2	2.28	1	2.35	12	2.37	118.7	105.8	135.1	0.5
Cu(21)	6	2.29	10	2.30	4	2.36	129.7	122.2	106.1	2.0
Cu(22)	9	2.25	3	2.30	10	2.36	140.9	108.7	107.9	2.6
Cu(23)	11	2.26	8	2.34	12	2.34	141.8	105.2	108.7	4.3
Cu(24)	2	2.29	12	2.33	7	2.34	125.5	124.3	109.4	0.8

[a] Plus $S(9)$ $d = 2.87$ Å

and Table 7 for djurleite. The difference from 360° of the sum of the S – Cu – S angles for the three shortest bonds is also given for each Cu atom as an indication of the degree of planarity of the CuS_3 group.

The distribution of the atoms in the two structures is represented schematically in Fig. 4, for low chalcocite in (a) and for djurleite in (b). The view is along the b axis for both, showing the hexagonal-close-packed sulfur layers on edge. In low chalcocite there is only one kind of layer but two kinds of interlayer copper arrangements. Djurleite contains two kinds of sulfur layer and three kinds of interlayer arrangement. An attempt is made in views normal to the sulfur layers to represent the geometry of these structures in sections as indicated in Fig. 4, two section being shown for low chalcocite in Fig. 5, and three sections for djurleite in Fig. 6. Figures 5 and 6 show that although many general features are shared in common between the two structures, there is no extensive analogy in detail.

Of the 24 Cu atoms in low chalcocite, 8 are located in the sulfur layers, occupying two thirds of the available triangular sites. The remaining Cu

Table 7. Cu – S interatomic distances and angles in djurleite. All distances less than 3.0 Å listed in increasing order of d. Last column gives the difference of the sum of 3 (largest) angles from full circle. Estimated standard deviation $\sigma(d) = 0.018$ Å, $\sigma(\phi) = 0.7$ deg

Atom	S_1	d_1	S_2	d_2	S_3	d_3	S_4	d_4	ϕ_{12}	ϕ_{23}	ϕ_{31}	360-$\Sigma\phi$
Cu(1)	14	2.29	15	2.31	3	2.34			121.4	112.2	126.1	0.2
Cu(2)	15	2.26	4	2.29	16	2.35			119.6	126.2	114.1	0.1
Cu(3)	5	2.27	2	2.32	1	2.37			123.4	126.0	109.6	1.0
Cu(4)	8	2.26	5	2.27	9	2.29			122.7	116.8	119.8	0.6
Cu(5)	10	2.28	5	2.30	6	2.32			116.9	121.2	120.5	1.4
Cu(6)	7	2.26	11	2.34	6	2.37			127.0	108.7	124.2	0.0
Cu(7)	9	2.30	10	2.30	13	2.30			111.8	115.6	131.6	1.0
Cu(8)	10	2.21	11	2.30	14	2.33			124.9	111.2	123.5	0.4
Cu(9)	11	2.30	15	2.31	12	2.36			126.3	112.6	120.6	0.5
Cu(10)	17	2.28	20	2.29	29	2.33			126.0	116.7	117.1	0.3
Cu(11)	17	2.24	30	2.26	18	2.35			121.5	116.4	121.0	1.1
Cu(12)	32	2.25	20	2.27	19	2.29			117.3	116.6	124.7	1.4
Cu(13)	21	2.20	17	2.23	22	2.49			121.7	122.4	115.9	0.0
Cu(14)	24	2.25	19	2.31	23	2.32			117.6	120.5	120.4	1.5
Cu(15)	24	2.27	20	2.27	21	2.35			121.1	116.9	122.0	0.0
Cu(16)	21	2.21	28	2.28	25	2.34			124.8	113.8	120.1	1.2
Cu(17)	24	2.25	28	2.28	27	2.33			119.6	121.5	118.4	0.5
Cu(18)	30	2.22	29	2.32	25	2.42			129.0	110.6	119.5	0.8
Cu(19)	30	2.28	26	2.31	31	2.32			117.6	126.7	115.6	0.0
Cu(20)	28	2.22	29	2.25	32	2.28			120.8	117.5	120.6	1.0
Cu(21)	16	2.30	13	2.31	2	2.36			131.6	106.9	118.7	2.8
Cu(22)	3	2.28	15	2.29	2	2.39			130.5	110.3	119.2	0.0
Cu(23)	14	2.26	4	2.27	3	2.30	15	2.95	123.9	113.2	118.5	4.4
Cu(24)	13	2.26	4	2.30	1	2.35			120.6	105.7	132.1	1.5
Cu(25)	2	2.31	6	2.31	12	2.32			115.8	122.2	121.7	0.2
Cu(26)	6	2.26	11	2.29	3	2.39			127.4	115.2	117.2	0.2
Cu(27)	10	2.28	4	2.40	7	2.43	8	2.61	114.1	102.2	133.8	9.9
Cu(28)	8	2.24	9	2.29	10	2.68	5	2.75	132.6	99.9	110.7	16.8
Cu(29)	7	2.21	6	2.31	11	2.59			130.3	102.6	123.5	3.6
Cu(30)	5	2.25	12	2.30	9	2.39			139.2	111.4	109.2	0.2
Cu(31)	1	2.24	16	2.33	9	2.37			134.9	105.9	117.9	1.3
Cu(32)	17	2.28	1	2.31	13	2.40			132.0	116.2	111.6	0.2
Cu(33)	18	2.25	2	2.35	14	2.38			131.2	108.8	119.7	0.4
Cu(34)	20	2.28	16	2.31	1	2.34			118.0	123.7	118.3	0.0
Cu(35)	23	2.25	7	2.28	3	2.31			121.4	108.6	128.6	1.4
Cu(36)	24	2.24	8	2.29	4	2.56	7	2.65	127.9	98.3	125.9	7.8
Cu(37)	8	2.28	21	2.28	1	2.31			131.1	115.7	112.3	0.9
Cu(38)	7	2.30	12	2.30	27	2.30			118.4	121.6	118.5	1.5
Cu(39)	28	2.27	8	2.29	12	2.30			118.5	118.2	123.0	0.2
Cu(40)	13	2.29	29	2.32	16	2.33			124.6	113.4	122.0	0.0
Cu(41)	30	2.28	13	2.29	14	2.34			128.3	111.2	119.3	1.2
Cu(42)	31	2.24	14	2.31	11	2.63			136.0	101.3	117.8	4.9
Cu(43)	32	2.24	12	2.29	16	2.29	15	2.99	119.6	108.6	125.8	6.0
Cu(44)	3	2.26	18	2.33	19	2.37			133.2	106.4	118.8	1.6
Cu(45)	4	2.24	19	2.30	20	2.69	24	2.90	135.2	101.6	112.2	11.1
Cu(46)	5	2.23	22	2.27	25	2.51			142.4	106.0	111.5	0.0

Table 7. (Continued)

Atom	S_1	d_1	S_2	d_2	S_3	d_3	S_4	d_4	ϕ_{12}	ϕ_{23}	ϕ_{31}	360-$\Sigma\phi$
Cu(47)	6	2.23	26	2.34	22	2.48	23	2.64	119.5	98.7	126.9	14.9
Cu(48)	9	2.26	25	2.44	29	2.56	28	2.62	122.6	102.4	115.9	19.1
Cu(49)	26	2.23	10	2.29	25	2.33			127.3	110.3	122.0	0.4
Cu(50)	11	2.26	27	2.28	26	2.29			130.3	113.9	115.1	0.7
Cu(51)	15	2.24	31	2.33	19	2.34			133.1	107.6	116.8	2.6
Cu(52)	24	2.28	18	2.30	22	2.32			122.5	123.5	111.6	2.4
Cu(53)	23	2.26	21	2.30	18	2.34			120.8	122.6	116.6	0.0
Cu(54)	19	2.23	22	2.44	25	2.50	21	2.80	121.6	100.9	124.2	13.2
Cu(55)	20	2.24	23	2.27	22	2.54	26	2.63	134.1	101.7	110.2	13.9
Cu(56)	17	2.26	27	2.29	23	2.31			116.8	112.9	129.1	1.2
Cu(57)	29	2.29	31	2.30	27	2.31			118.6	116.2	125.1	0.1
Cu(58)	30	2.26	27	2.30	32	2.30			129.7	115.7	114.0	0.6
Cu(59)	28	2.26	18	2.29	31	2.29	30	2.99	121.4	113.0	121.9	3.7
Cu(60)	25	2.27	32	2.33	31	2.36			130.0	110.3	118.3	1.4
Cu(61)	26	2.26	32	2.30	20	2.62	29	2.90	132.2	103.1	115.1	9.6
Cu(62)	22	2.19	2	2.20					172.2			

atoms are located between the layers, mostly in triangular sites, though some are highly distorted. One atom, Cu(14) is shifted strongly out of the triangular plane toward a fourth S atom, thus approaching a severely distorted tetrahedral environment. The two atoms that were divided in the structure analysis described earlier, Cu(15) and Cu(19), both show a strong inclination toward twofold, linear coordination. In the attempted split-atom refinement, in each case one half of the atoms moved to an essentially linear, twofold site with Cu – S distances averaging 2.16 Å, while the other half took an adjacent, highly distorted triangular position. In djurleite, 51 Cu atoms lie in more or less distorted triangles, 9 approach tetrahedral coordination (including Cu – S distances to 2.95 Å) although highly distorted, and one, Cu(62), is in unique linear, twofold coordination. For the last atom the bond lengths are 2.19 Å and the angle between the bonds is 172°. In low chalcocite the average Cu – S distances within the 21 CuS_3 groups is 2.32 Å, and in djurleite the average within the 51 CuS_3 groups is 2.29 Å. These distances may be compared with the triangular bonds in covellite, 2.19 Å, and stromeyerite, 2.26 Å.

Each copper atom in low chalcocite and djurleite has from 2 to 8 other copper atom neighbors closer than 3.0 Å. The Cu – Cu distances in low chalcocite (given in Table 8) vary upward from 2.46 Å with a pronounced clustering between 2.7 and 2.8 Å. Among the Cu – Cu distances in djurleite (listed in Table 9) the shortest is 2.45 Å, and again a population maximum appears between 2.7 and 2.8 Å. Covellite and stromeyerite have no Cu – Cu

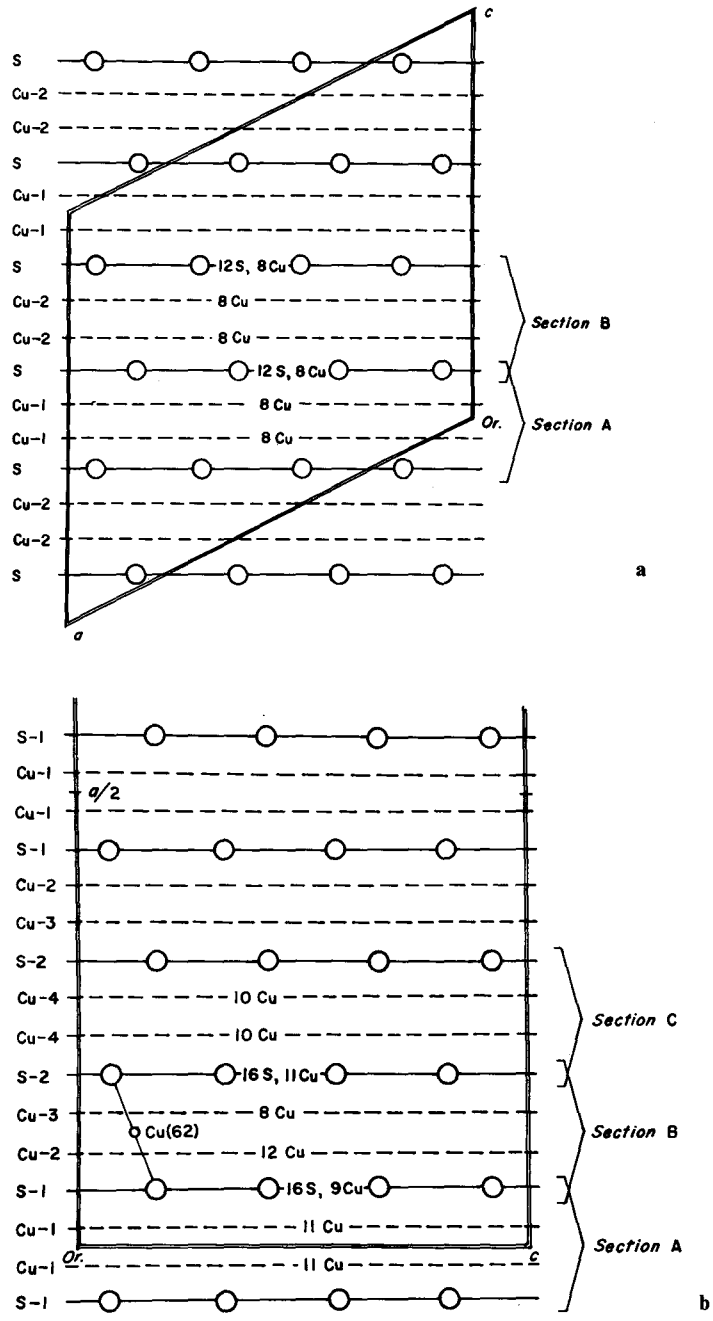

Fig. 4. Distribution of atoms in low chalcocite (a) and djurleite (b), shown schematically as viewed along the *b* axes

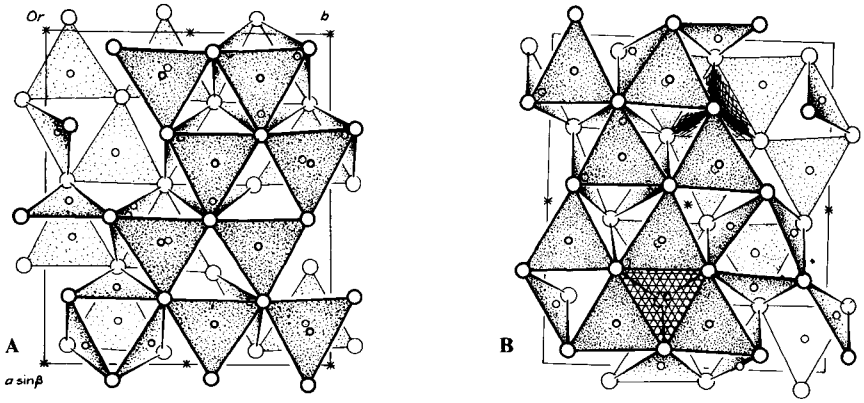

Fig. 5. Projected sections A and B (as indicated in Fig. 4a) of the low chalcocite structure, in which CuS_3 groups are shown as shaded triangles, distorted CuS_4 groups as line-hatched tetrahedra

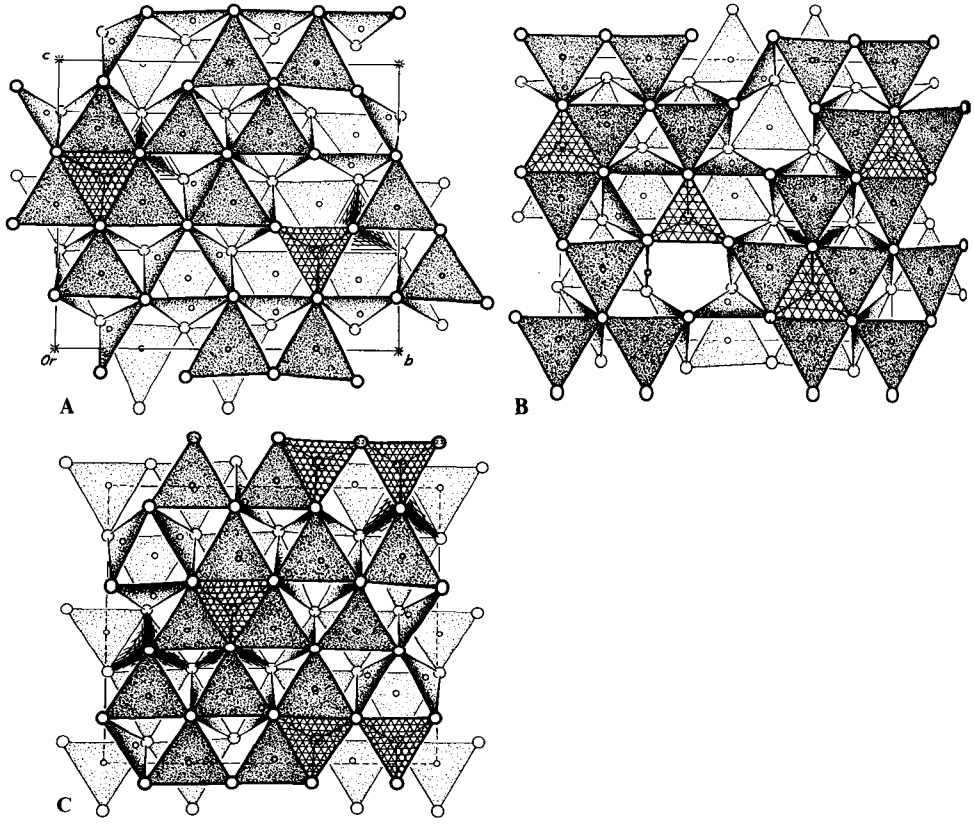

Fig. 6. Projected sections A, B and C (as indicated in Fig. 4b) of the djurleite structure, with triangles and tetrahedra represented as in Fig. 5

Table 8. Cu – Cu interatomic distances in low chalcocite. All distances less than 3.0 Å are listed in increasing order of d. Standard deviations $\sigma(d) = 0.007$ Å

Atom	Cu	d	Cu	d	Cu	d	Cu	d	Cu	d	Cu	d
Cu(1)	15	2.65	9	2.69	14	2.74	7	2.85	13	2.87	8	2.93
Cu(2)	19	2.64	18	2.68	11	2.72	22	2.79	16	2.80		
Cu(3)	14	2.66	16	2.72	21	2.99						
Cu(4)	19	2.66	12	2.71	18	2.75	10	2.86	11	2.89	17	2.91[a]
Cu(5)	15	2.58	23	2.76	18	2.82	7	2.90	20	2.98		
Cu(6)	13	2.76	20	2.76	8	2.86	17	2.92				
Cu(7)	20	2.77	9	2.80	8	2.81	1	2.85	5	2.90		
Cu(8)	9	2.78	7	2.81	24	2.83	6	2.86	1	2.93		
Cu(9)	1	2.69	22	2.69	8	2.78	7	2.80	21	2.98		
Cu(10)	21	2.69	11	2.74	12	2.74	4	2.86				
Cu(11)	2	2.73	10	2.74	12	2.84	16	2.87	4	2.89		
Cu(12)	23	2.68	4	2.71	10	2.74	24	2.81	11	2.84		
Cu(13)	22	2.60	6	2.76	20	2.85	1	2.87				
Cu(14)	3	2.66	24	2.68	1	2.74	21	2.88				
Cu(15)	5	2.58	20	2.59	1	2.65	24	2.75				
Cu(16)	19	2.60	3	2.72	2	2.80	18	2.82	11	2.87		
Cu(17)	4	2.91	6	2.92								
Cu(18)	23	2.52	21	2.60	2	2.68	4	2.75	5	2.82	16	2.82
Cu(19)	16	2.60	2	2.64	4	2.66	21	2.73				
Cu(20)	15	2.59	6	2.76	7	2.77	13	2.85	5	2.98		
Cu(21)	18	2.60	10	2.69	19	2.73	22	2.82	14	2.88	9	2.98[b]
Cu(22)	13	2.60	9	2.69	2	2.79	21	2.82				
Cu(23)	18	2.52	12	2.68	24	2.73	5	2.78	4	2.98		
Cu(24)	14	2.68	23	2.73	15	2.75	12	2.81	8	2.83		

[a] Plus: 23 2.98
[b] Plus: 3 2.99

Table 9. Cu – Cu interatomic distances in djurleite. All distances less than 3.0 Å are listed in increasing order of d. Estimated standard deviation $\sigma(d) = 0.014$ Å

Atom	Cu	d	Cu	d	Cu	d	Cu	d	Cu	d	Cu	d
Cu(1)	42	2.73	22	2.74	44	2.74	23	2.90	33	2.90	51	2.90
Cu(2)	21	2.75	23	2.75	34	2.75	24	2.80	45	2.80	43	2.87
Cu(3)	62	2.67	32	2.72	31	2.76	30	2.77	21	2.81	25	2.99
Cu(4)	28	2.64	37	2.72	39	2.84	28	2.87				
Cu(5)	46	2.72	29	2.73	28	2.75	49	2.84	25	2.94		
Cu(6)	29	2.54	29	2.70	50	2.71	35	2.77	38	2.78	26	2.80
Cu(7)	40	2.60	28	2.67	24	2.72	31	2.79	41	2.89	48	2.93
Cu(8)	42	2.55	41	2.79	23	2.80	27	2.83	29	2.85		
Cu(9)	22	2.73	26	2.77	42	2.78	25	2.80	43	2.86	38	2.90
Cu(10)	32	2.71	40	2.71	56	2.73	34	2.77	61	2.87	55	2.98
Cu(11)	59	2.75	41	2.79	52	2.79	33	2.86				
Cu(12)	45	2.45	61	2.47	51	2.66	60	2.77				
Cu(13)	62	2.69	54	2.79	52	2.82	46	2.90				